OPEN ACCESS
Advances in Animal and Veterinary Sciences

Research Article

Identification of Normal Horse Head Structures, with Special Reference to Paranasal Sinuses, by Anatomical Cross-section and Magnetic Resonance Imaging (MRI)

Mohamed Aref[1], Ahmed Abdelbaset-Ismail[2*], Hassan Emam[1], Kuldeep Dhama[3]

[1]Department of Anatomy and Embryology, Faculty of Veterinary Medicine, Zagazig University, Zagazig, El-Sharkia, Egypt; [2]Department of Surgery, Radiology and Anaesthesiology, Faculty of Veterinary Medicine, Zagazig University, Zagazig, El-Sharkia, Egypt. [3]Division of Pathology, ICAR-Indian Veterinary Research Institute, Izatnagar, India.

Abstract | The purpose of this report was to describe the axial appearance of the normal horse head with special reference to the paranasal sinuses using magnetic resonance imaging (MRI) technique and anatomical cross sections. In order to do this, T1 (longitudinal relaxation time)-weighted, 1cm –thick images of horse cadaver heads (n=5) were captured using closed magnet of a 1-Tesla (field strength). Afterwards, the frozen heads were cross-sectionally sliced at seven planes (from the level of upper and lower incisors to the level of perpendicular plate of ethmoidal bone) according to MRI slices thickness, and then correspondingly compared with the MRI images. The obtained data (per each plane) properly defined the normal anatomical features of the normal horse head by both anatomical cross-sections and MR images. The MR images from this investigation provided a clear definition of normal horse head structures and were consistent with that of gross anatomical sections. The T1-weighted images showed that the mineral-rich tissues (bones and teeth) appeared dark (no signal), cartilages and muscles appeared grey (low signal intensity, hypointense), and fat (subcutaneous and within bone marrow) appeared bright (high signal, hyperintense). The air-containing sinuses and conchae appeared dark without signals. As this study demonstrates normal horse head structures with a particular attention to nasal cavity structures and its relation to five types of paranasal sinuses, it could be used as a landmark and reference to properly diagnose various surgical disorders of head region particularly paranasal sinuses that are the most common in horses.

Keywords | MRI, Anatomy, Head, Horse, Cross-section, Surgery

Editor | Kuldeep Dhama, Indian Veterinary Research Institute, Uttar Pradesh, India.
Received | November 14, 2018; **Accepted** | December 01, 2018; **Published** | December 29, 2018
***Correspondence** | Ahmed Abdelbaset-Ismail, Department of Surgery, Radiology and Anaesthesiology, Faculty of Veterinary Medicine, Zagazig University, Zagazig, El-Sharkia, Egypt; **Email**: a4ismail@yahoo.co.uk.
Citation | Aref M, Ismail AA, Emam H, Dhama K (2019). Identification of normal horse head structures, with special reference to paranasal sinuses, by anatomical cross-section and magnetic resonance imaging (mri). Adv. Anim. Vet. Sci. 7(3): 200-204.
DOI | http://dx.doi.org/10.17582/journal.aavs/2019/7.3.200.204
ISSN (Online) | 2307-8316; **ISSN (Print)** | 2309-3331

Copyright © 2019 Aref et al. This is an open access article distributed under the Creative Commons Attribution License, which permits unrestricted use, distribution, and reproduction in any medium, provided the original work is properly cited.

INTRODUCTION

It is well known that magnetic resonance imaging (MRI) of the horse is technically difficult due to lack of a large fitting magnetom, therefore, its use is only limited to the cadavers examination (Dyson et al., 2003; Liuti et al., 2017). The anatomical complexity of the horse head region, makes it an area of homing of many pathological and surgical lesions that definitely require new techniques, i.e., MRI to reach an exact diagnosis (Tessier et al., 2013; Pease et al., 2017). Superimposition of the anatomical structures, and the presence of the osseous coverage of head and gas-containing sinuses lead to confounding interpretation of radiography and blurring ultrasonographic view, respectively (Park 1993; Weller et al., 1999; Tucker and Farrell 2001). In this regards, there is limited information about the use of MRI combining with cross-sectional anatomy of normal equine paranasal sinuses (Arencibia et al., 2000) and brain (Chaffin et al., 1997; Arencibia et al., 2001). MR imaging has been extensively used for critical evaluation and subsequently ultimate diagnosis of various acquired or congenital disorders of human, feline and canine head

(Parslow et al., 2016; Huizing et al., 2017), however, only few studies in which MRI was used for diagnosis of head disorders in horses (Manso-Diaz et al., 2015). Therefore, all these results provide potential evidence regarding the importance of such technique for both earlier detection of neurological, sino-nasal, and soft-tissue disorders (Tessier et al., 2013; Manso-Diaz et al., 2015) and establishing the treatment strategy. The aim of this investigation was to provide a detailed description of the normal horse head structures by cross-sectional anatomy and MR imaging.

MATERIALS AND METHODS

Cadaver heads (n=5) employed in this study were harvested from normal adult horses of mixed breeds (6-years ± 9-months-old). This study was performed at Faculty of Veterinary Medicine, Zagazig University, and all conducted procedures were fulfilled according to the institutional guidelines for regulation of the care and use of animals. The horses were euthanized due to incurable diseases unrelated to the head region. The heads were kept cooled and scanned within 4-hours after euthanasia. Each head was scanned using MRI machine (Philips, Intra, USA) of 1-tesla field strength of internal magnetom and human body coil. The T1 (longitudinal relaxation time)-weighted transverse plane produced by using short time to echo (TE) and repetition time (TR) was performed. After imaging, the heads were kept frozen at -15°C and then cross-sectionally sliced by an electrical saw at the same scanning points of transverse plane used during MRI examination. The cross-sectional slicing was done at seven different levels: at the level of upper and lower incisors, the body of mandible, the first and second premolar teeth, the third premolar tooth, the molar teeth, the diastema, and the perpendicular plate of ethmoidal bone. Each obtained section was thoroughly cleaned and photographic image was captured, labeled and then compared for matching with its relevant transverse MR image to assure the corresponding anatomic features.

RESULTS

The representative seven MR images and their relevant cross-sections of the normal structures of the equine nasal cavity and their paranasal sinuses from the level of upper and lower incisors to the level of perpendicular plate of ethmoidal bone are depicted in Figures 1, 2, 3, 4, 5, 6 and 7. It is clear from the figures that dorsal, middle, ventral and ethmoidal nasal conchae divide the nasal cavity into different air meatuses: dorsal, middle, ventral and common nasal meatuses. Dorsal nasal concha has straight fold, while ventral nasal concha has alar fold and basal fold. Both last conchae are organized rostrally as recess and caudally as sinus. Middle and ethmoid nasal conchae appeared small and undivided. The both maxillary sinuses are divided into rostral maxillary sinus and caudal maxillary sinus. The two frontal sinuses occupy the dorsal part directly below the frontal bone and are divided by a bony septum. Dorsal and ventral conchal sinuses occupy the caudal part of the dorsal and ventral nasal concha. Concho-frontal sinus is an extension of frontal sinus and communicates with the sinus of the dorsal nasal concha. The concho-frontal sinus communicates with the caudal maxillary sinus by an opening termed fronto-maxillary opening. Sphenopalatine sinuses are the smallest sinuses and located in the body of sphenoid (Figures 1, 2, 3, 4, 5, 6 and 7).

Herein by MR imaging, we found that mineral-rich tissues (bones and teeth) appeared dark (no signal). Cartilages and muscles appeared grey (low signal intensity, hypointense), while fat (subcutaneous and within bone marrow) appeared bright (high signal, hyperintense). The air-containing sinuses and conchae appeared dark without signals.

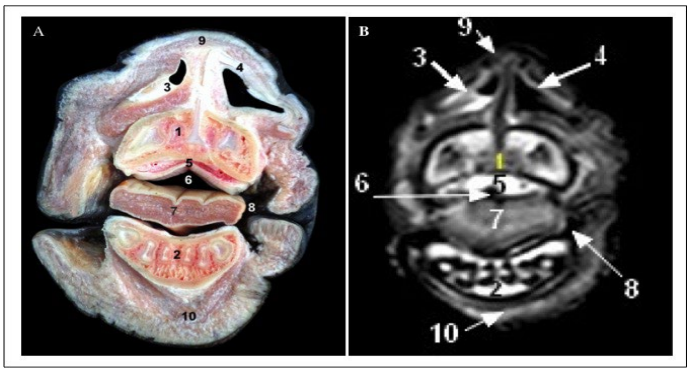

Figure 1: Cross sectional anatomy (Panel A) and MR image (Panel B) of horse head at the level of upper and lower incisors. 1) Upper incisors teeth; 2) Lower incisors teeth; 3) plate of alar cartilage; 4) Horn of alar cartilage; 5) Hard palate; 6) Oral cavity proper; 7) Apex of tongue; 8) Labial vestibule; 9) Apical naris dilatator muscle; 10) Mentalis muscle.

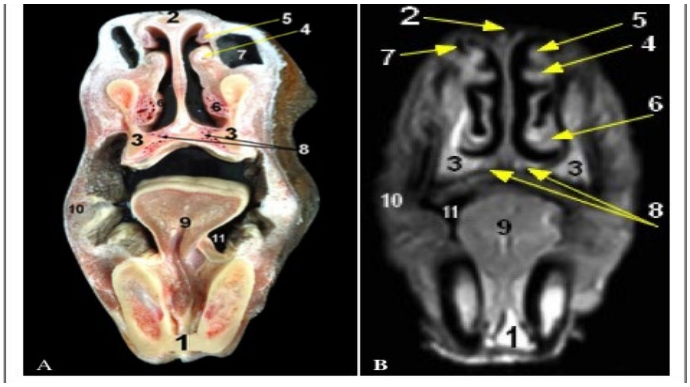

Figure 2: Cross sectional anatomy (Panel A) and MR image (Panel B) of horse head at the level of body of mandible. 1) Body of mandible; 2) Nasal bone; 3) Maxilla bone; 4) medial accessory nasal cartilage at Alar fold; 5) Straight fold; 6) Basal fold; 7) False nostril (Nasal diverticulum);

8) Vomeronasal organ; 9) Tongue; 10) Buccinators muscle; 11) Sublingual recess.

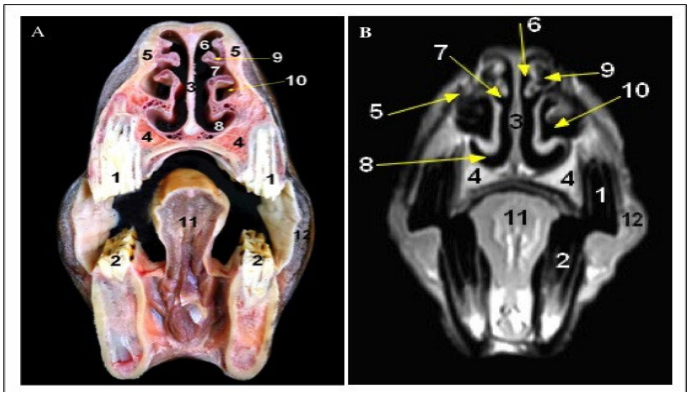

Figure 3: Cross sectional anatomy (Panel A) and MR image (Panel B) of horse head at the level of first and second premolar teeth. 1) Upper first and second premolar teeth; 2) Lower first and second premolar teeth; 3) Cartilaginous part of Nasal septum; 4) maxilla bone; 5) Nasal bone; 6) Dorsal nasal meatus; 7) Middle nasal meatus; 8) Ventral nasal meatus; 9) Dorsal nasal concha; 10) Ventral concha1 bulla; 11) Body of tongue; 12) Buccinators muscle.

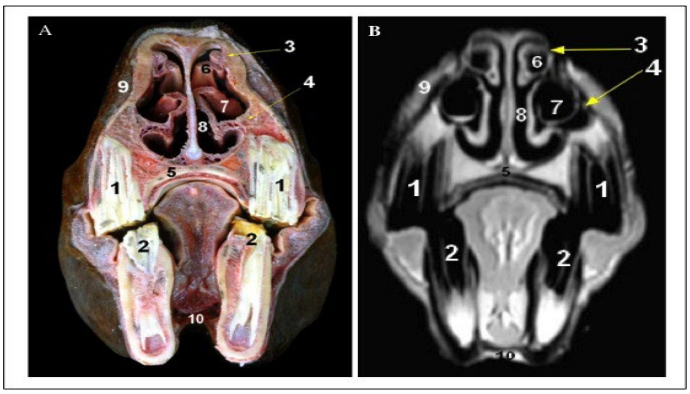

Figure 4: Cross sectional anatomy (Panel A) and MR image (Panel B) of horse head at the level of the third premolar tooth**.** 1) Upper third premolar tooth; 2) Lower third premolar tooth; 3) Dorsal turbinate crest of Nasal bone; 4) Ventral turbinate crest of maxilla bone; 5) Palatine process of Maxilla; 6) Dorsal nasal concha; 7) Ventral nasal concha (bulla); 8) Common nasal meatus; 9) Superior labii levator muscle; 10) Geniohyoid muscle.

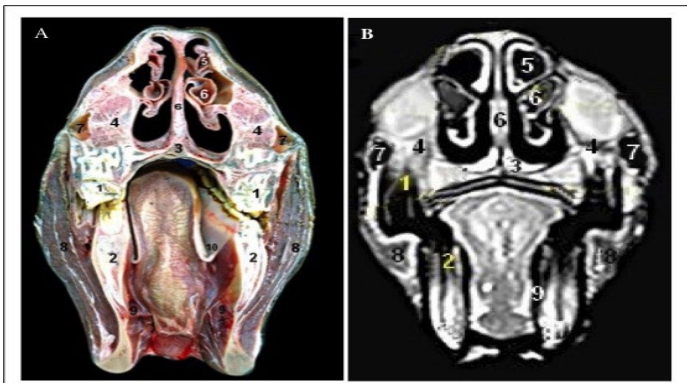

Figure 5: Cross sectional anatomy (Panel A) and MR image (Panel B) of horse head at the level of the molar teeth. 1) Upper molar teeth; 2) Lower molar teeth; 3) Vomer; 4) Maxilla bone; 5) Dorsal conchal bulla; 6) Ventral conchal sinus; 7) Rostral maxillary sinus; 8) Masseter muscle; 9) Pteyrgoid muscle (medial part); 10) Palatoglossal fold.

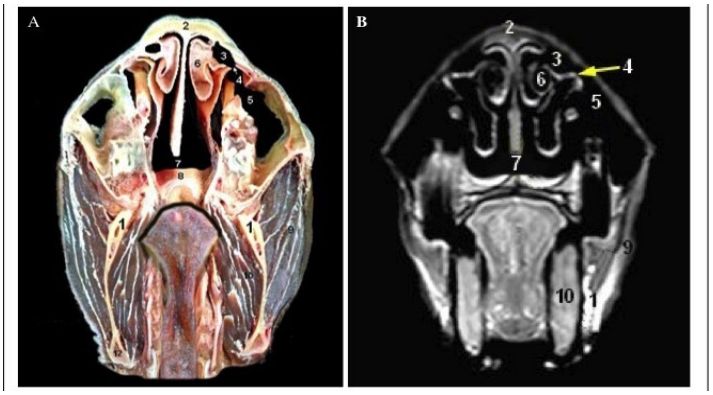

Figure 6: Cross sectional anatomy (Panel A) and MR image (Panel B) of horse head at the level of the diastema. 1) Ramus of mandible; 2) Nasal bone; 3) Concho frontal sinus (rostral part); 4) Fronto-maxillary opening; 5) Caudal maxillary sinus; 6) Dorsal nasal sinus (Caudal end of dorsal nasal concha); 7) Nasopharynx; 8) Soft palate; 9) Masseter muscle; 10) Pteyrgoid muscle (medial part).

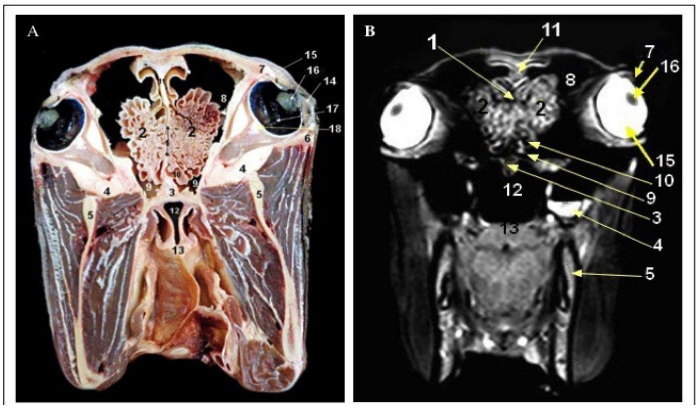

Figure 7: Cross sectional anatomy (Panel A) and MR image (Panel B) of horse head at the level of the perpendicular plate of ethmoidal bone**.**1) Perpendicular plate of ethmoidal bone; 2) Ethmoid labyrinth (ethmoid conchae); 3) Vomer bone; 4) Maxilla; 5) Mandible; 6) Zygomatic arch; 7) Orbit; 8) Conchofrontal sinus (caudal part); 9) Sphenopalatine sinus; 10) Middle conchal sinus; 11) Septum of frontal sinus; 12) Nasopharynx; 13) Soft palate; 14) cornea; 15) Sclera; 16) Lens; 17) Retina; 18) Extra-ocular muscles.

DISCUSSION

From the surgical and anatomical point of view it is worthy to combine the computed imaging techniques such as computed tomography (CT) and magnetic resonance imaging (MRI) with the cross-sectional anatomy for better understanding the normal body structures (Arencibia et al.,

2000). As well, by this approach, a clear visualization and identification of the complex and super imposed structures (as in case of head region) can also be achieved. It is well known that the MRI is a beneficial diagnostic tool for clear discrimination the soft tissues from the mineral-rich tissues and gas-containing sacs particularly of complex-structured areas (Arencibia et al., 2000). The head area is considered as a good example for studying MRI because its anatomical complexity (Pease et al., 2017). Superimposition of head structures and presence of skull hinder the specific interpretation in case of radiography and improper sonic waves penetration in case of ultrasonography, respectively (Park 1993; Weller et al., 1999). Previous study has reported that computed tomography assists in identification of para-nasal sinuses of cadaver heads of adult horses (De Zani et al., 2010). Additionally, these sinuses as well as brain have been assessed in a normal and diseased condition by anatomical and MR imaging in horse (Chaffin et al., 1997; Arencibia et al., 2000; Arencibia et al., 2001; Cavalleri et al., 2013; Manso-Diaz et al., 2015). Hence, it was worthy to expand the limited information about normal anatomical structures of adult horse head by MRI. Since MRI is described by its superior contrast resolution particularly for soft tissues, the various structures of horse head, as shown herein, were clearly detailed using T1-weighted MRI in parallel with the cross-section anatomy. MRI is essential to properly diagnose various head disorders such as tumors, cysts, ethmoid and hematoma (Manso-Diaz et al., 2015). Although the availability of using MRI in horses is yet limited, future designation of its open magnet to fit horse size may become available due to its essential role for diagnostic purposes in such worthy animal, horse. In the current study, we found that the T1-relaxation time is reversibly correlated with the signal intensity (Arencibia et al., 2000). Hence by using this type of scan, the higher intensities (fats), hypointensities (muscles and cartilages), and lower intensities (bones, and air-containing sinuses) structures could be clearly visualized.

CONCLUSION

We could concluded that this study might constitute as landmark to assist in the proper evaluation of the normal and abnormal structures of the equine head with a particular attention to paranasal sinuses by using MR imaging.

ACKNOWLEDGEMENTS

This work was supported by Faculty of Veterinary Medicine, Zagazig University, Egypt.

CONFLICT OF INTEREST

The authors declare that no competing interest exists.

AUTHORS CONTRIBUTION

This study was completed by a proportionate contribution of all authors.

REFERENCES

- Arencibia A, Vazquez JM, Jaber R, Gil F, Ramirez JA, Rivero M, Gonzalez N, Wisner ER (2000). Magnetic resonance imaging and cross sectional anatomy of the normal equine sinuses and nasal passages. Vet. Radiol. Ultrasound. 41(4): 313-319. https://doi.org/10.1111/j.1740-8261.2000.tb02079.x
- Arencibia A, Vazquez JM, Ramirez JA, Ramirez G, Vilar JM, Rivero MA, Alayon S, Gil F (2001). Magnetic resonance imaging of the normal equine brain. Vet. Radiol. Ultrasound.42(5): 405-409. https://doi.org/10.1111/j.1740-8261.2001.tb00959.x
- Cavalleri JM, Metzger J, Hellige M, Lampe V, Stuckenschneider K, Tipold A, Beineke A, Becker K, Distl O, Feige K (2013). Morphometric magnetic resonance imaging and genetic testing in cerebellar abiotrophy in Arabian horses. BMC Vet. Res. 9: 105. https://doi.org/10.1186/1746-6148-9-105
- Chaffin MK, Walker MA, McArthur NH, Perris EE, Matthews NS (1997). Magnetic resonance imaging of the brain of normal neonatal foals. Vet. Radiol.Ultrasound. 38 (2): 102-11. https://doi.org/10.1111/j.1740-8261.1997.tb00823.x
- De Zani D, Borgonovo S, Biggi M, Vignati S, Scandella M, Lazzaretti S, Modina S, Zani D (2010). Topographic comparative study of paranasal sinuses in adult horses by computed tomography, sinuscopy, and sectional anatomy. Vet. Res. Commun. 34 Suppl 1: S13-16. https://doi.org/10.1007/s11259-010-9381-6
- Dyson S, Murray R, Schramme M,Branch M (2003). Magnetic resonance imaging of the equine foot: 15 horses. Equine Vet. J.35 (1): 18-26. https://doi.org/10.2746/042516403775467531
- Huizing X, Sparkes A, Dennis R (2017). Shape of the feline cerebellum and occipital bone related to breed on MRI of 200 cats. J. Feline Med. Surg. 19 (10): 1065-1072. https://doi.org/10.1177/1098612X16676022
- Liuti T, Smith S, Dixon PM (2017). A Comparison of Computed Tomographic, Radiographic, Gross and Histological, Dental, and Alveolar Findings in 30 Abnormal Cheek Teeth from Equine Cadavers. Front. Vet. Sci. 4: 236. https://doi.org/10.3389/fvets.2017.00236
- Manso-Diaz G, Dyson SJ, Dennis R, Garcia-Lopez JM, Biggi M, Garcia-Real MI, San Roman F, Taeymans O (2015). Magnetic resonance imaging characteristics of equine head disorders: 84 cases (2000-2013). Vet. Radiol. Ultrasound 56 (2): 176-187. https://doi.org/10.1111/vru.12210
- Park RD (1993). Radiographic examination of the equine head. Vet. Clin. North. Am. Equine Pract. 9 (1): 49-74. https://doi.org/10.1016/S0749-0739(17)30415-7
- Parslow A, Taylor DP,Simpson DJ (2016). Clinical, computed tomographic, magnetic resonance imaging, and histologic findings associated with myxomatous neoplasia of the temporomandibular joint in two dogs. J. Am. Vet. Med. Assoc. 249 (11): 1301-1307. https://doi.org/10.2460/javma.249.11.1301
- Pease A, Mair T,Spriet M (2017). Imaging the equine head and spine. Equine Vet. J.49 (1): 13-4. https://doi.org/10.1111/

evj.12640
- Tessier C, Bruhschwein A, Lang J, Konar M, Wilke M, Brehm W, Kircher P (2013). Magnetic resonance imaging features of sinonasal disorders in horses. Vet. Radiol. Ultrasound. 54 (1): 54-60. https://doi.org/10.1111/j.1740-8261.2012.01975.x
- Tucker RL, Farrell E (2001). Computed tomography and magnetic resonance imaging of the equine head. Vet. Clin. North. Am. Equine Pract. 17 (1): 131-144. https://doi.org/10.1016/S0749-0739(17)30079-2
- Weller R, Cauvin ER, Bowen IM, May SA (1999). Comparison of radiography, scintigraphy and ultrasonography in the diagnosis of a case of temporomandibular joint arthropathy in a horse. Vet. Rec.144 (14): 377-379. https://doi.org/10.1136/vr.144.14.377